Geolological Survey Professional Paper 800-C, p. C71-C78.
Nicholson, G.E., 1990, Structural overview of Elk Hills, *in* Kuespert, J.G., and Reid, S.A., eds., Structure, Stratigraphy and Hydrocarbon Occurrences of the San Joaquin Basin, California, Pacific Section, SEPM, Book 64, p.133-140.
Selley, R.C., 1985, Elements of Petroleum Geology: New York, W.H. Freeman and Co., 449 p.
Webb, G.W., (1981) Stevens and earlier Miocene tubidite sandstones, southern San Joaquin valley, California: American Association of Petreoleum Geologists Bulletin v. 65, p. 438-465.
Woodring, W.P, Roundy, P.V., and Farnsworth, H.R., 1932, Geology and oil resources of the Elk Hills, California: U.S. Geological Survey Bulletin 835, 82 p.

ANALYSIS OF FAULT AND FRACTURE DATA FROM THE SAN ANDREAS FAULT, TOMS POINT, POINT REYES, CALIFORNIA

Anna Sojourner
Woodward-Clyde Federal Services
500 12th Street, Suite 200
Oakland, CA 94607

Karen Grove
Department of Geosciences
San Francisco State University
1600 Holloway Ave.
San Francisco, CA 94132

ABSTRACT

The San Andreas fault cuts through Toms Point, located on the northeastern edge of Tomales Bay, where active fault strands were observed following the great 1906 San Francisco earthquake. Tomales Bay, approximately 80 km north of San Francisco, is a linear depression created by the San Andreas fault. Toms Point consists of Franciscan Complex basement rock overlain by a nearly 30-m-thick sequence of coastal sediments of the Millerton Formation. The Millerton Formation is estimated by thermoluminescence dating to have an age of 132±12 ka.

Fracture and fault data measured within the Millerton Formation on Toms Point were used to correlate features observed on the northwest side with features from the southeast side and to estimate the state of stress along the San Andreas fault.

Cross sections of the northwest and southeast sides demonstrate the continuity of sediments through the Toms Point headland. Fault strands which are clearly exposed on the northwest side of Toms Point are covered on the southeast side, and their continuity is inferred by a linear topographic low along the crest of the headland which projects into a covered interval on the southeast side.

Fracture data collected at Toms Point are consistent with the state of stress measured at other locations along the San Andreas fault. Some fractures are extension fractures with plumose structures, and others are consistent with R and R' Reidel shears, at ± 45° from the direction of the maximum principal stress. Conjugate fractures in the youngest sediments at Toms Point may record a local extensional event, possibly caused by a right stepover between fault strands.

INTRODUCTION

Many features associated with the San Andreas fault (SAF) were first observed near Point Reyes. Large offsets from the 1906 San Francisco earthquake were documented throughout the area; the maximum horizontal offset of nearly 5 m was measured near the town of Olema (Fig 1). At the Toms Point study area, horizontal offset of nearly 2.5 m was measured by Lawson (1908).

Toms Point is located along the northeastern edge of Tomales Bay (Fig. 2). Tomales Bay lies approximately 80 km north of San Francisco and is a linear depression whose trend coincides with the SAF. At Tomales Bay, the SAF juxtaposes the Franciscan Complex with plutonic and metamorphic rock of the Salinian terrane. Toms Point consists of Franciscan basement rock overlain by the Pleistocene Millerton Formation, which is found in scattered outcrops along the eastern edge of Tomales Bay (Fig. 2).

Toms Point, a small headland bisected by the SAF (Fig. 3), is of particular geologic interest because the cliffs on the northwest side offer a direct view of active fault traces, previously mapped as two en echelon segments (Brown and Wolfe, 1970, Blake *et al.*, 1974).

This report presents fault and fracture data that are used to interpret the deformation visible at Toms Point and to correlate exposures on the northwest and southeast sides of the headland. A cross section of the exposures on the southeast side was interpreted in combination with a cross section of the northwest exposures from Rutledge (1993). Fracture orientations were collected with a Brunton compass and plotted using a stereonet plotting program (Allmendinger, 1995). The relationships of fault strands, their topographic expressions, and the stresses inferred from fracture orientations help to understand the deformation at Toms Point in the context of the geologic setting of coastal California.

STRATIGRAPHY OF THE MILLERTON FORMATION

Toms Point is the location of one of a few exposures of the Millerton Formation along the eastern edge of Tomales Bay. These exposures, which occur at Tomasini Point, Millerton Point, and Toms Point, are erosional remnants of the Millerton Formation (Fig. 2). The Millerton Formation at Toms Point forms a south-plunging anticline, with the SAF parallel to its axis (Fig. 3).

In Gary H. Girty, Richard E. Hanson, and John D. Cooper, Eds., 1997, **Geology of The Western Cordillera: Perspectives from Undergraduate Research.** Pacific Section S.E.P.M, Vol. 82, p. 57-64.

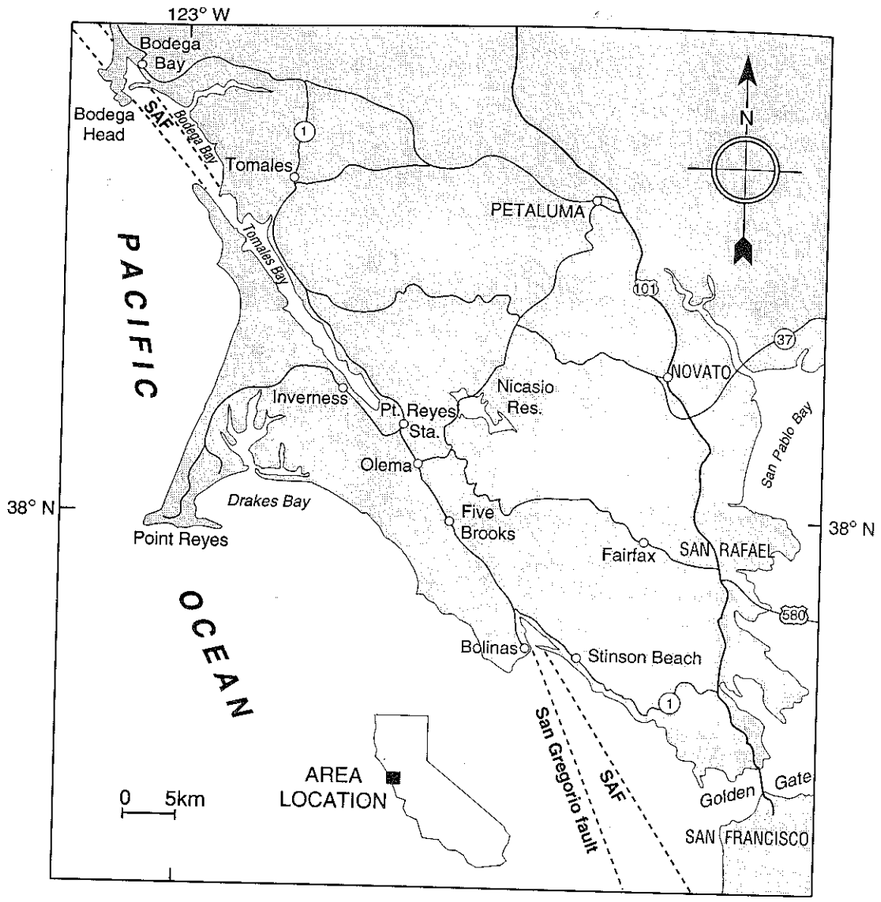

Figure 1. Location map, from Grove et al., 1995. SAF=San Andreas fault.

rounded. Clasts are largely of Franciscan origin, but some were derived from Salinian granite.

The mud and muddy sand were deposited in an estuarine or tidal environment. The gravel is fluvial in origin, and was deposited at times of lower sea level. Several angular unconformities separate transgressive sequences that fine upward from river gravel to estuarine mud. Unconformably overlying these sequences are massive dune sand deposits.

THE SAN ANDREAS FAULT

The SAF zone is typically up to several km wide, and is composed of many parallel strands (Wallace, 1990). The maximum principal stress for the SAF is nearly perpendicular to the fault, at approximately 033°, producing fault-normal compression in western California (Zoback *et al.*, 1987). This component of compression is responsible for much of the deformation and raised topography along the California coast.

The Millerton Formation consists of coastal sediments that were deposited at 132 ± 12 ka (Grove *et al.*, 1995) in estuarine, fluvial, and eolian environments. Mud, muddy sand, sand and gravel make up the Millerton Formation. The mud layers are gray and highly fractured. Some of the mud is sandy and laminated. Sand in the estuarine sequences is plane bedded and contains some mud, and is more consolidated than the younger massive dune sand. The massive sand consists of well-sorted, well-rounded, fine- to medium-sized quartz and feldspar grains. The sand is beige where unweathered, but weathers to yellow or dark orange where close to the overlying soil. The weathering pattern is uneven, perhaps because of permeability differences where the sediment has been bioturbated by plant roots and animal burrowing. Gravel layers have lenticular shapes and are internally cross-bedded. The gravel has a matrix of orange-weathered sand with some clay. The clasts are of variable size, from pebbles to cobbles, and are well-

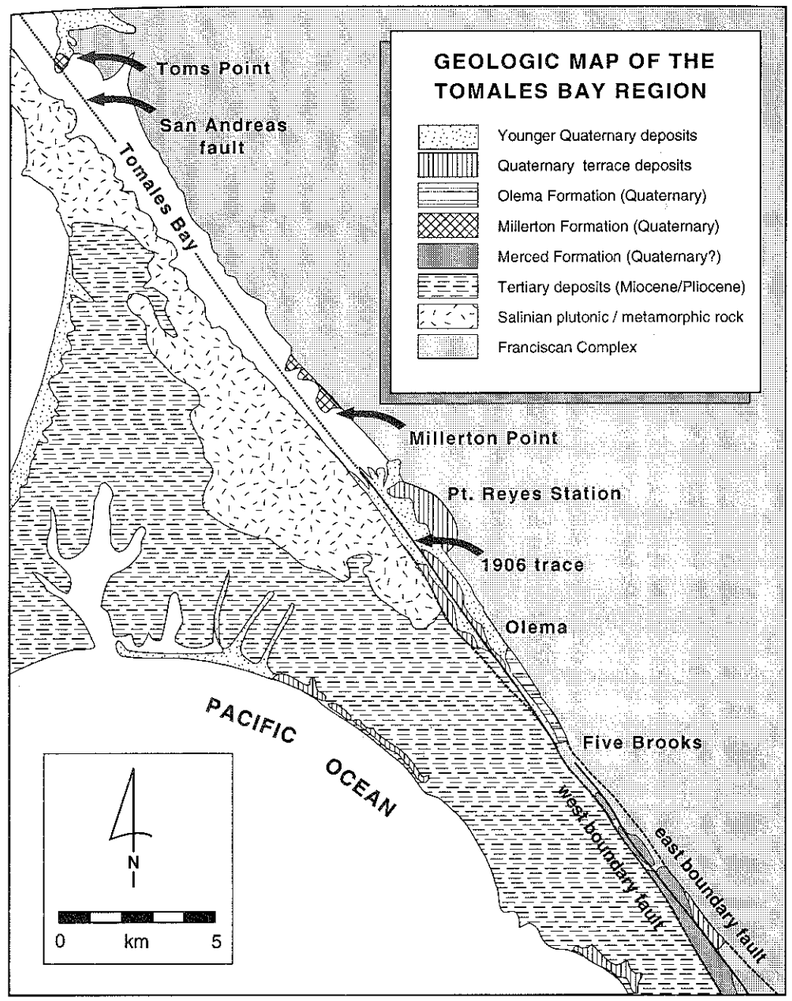

Figure 2. Generalized geologic map for the Tomales Bay region. Geology adapted from Galloway (1979).

FAULT DATA AND INTERPRETATION

Figure 3 shows the locations of cross sections and inferred fault strands on Toms Point. On the northwest side of Toms Point, three major fault strands are visible. In contrast, the faults are covered by vegetation and slump deposits on the southeast side. Descriptions of the outcrops on either side of the headland follow.

Northwest Side

Three strands of the San Andreas fault are exposed on the northwest side of Toms Point. Figure 3 shows the location of the easternmost and westernmost strands in map view. Figure 4, adapted from Rutledge (1993), shows how sediments are deformed between these strands.

At the northeast end of this cross section lie mud, sand and gravel of the Millerton Formation in a sequence very similar to the sedimentary sequence seen on the southeast side of Toms Point. To the northeast,

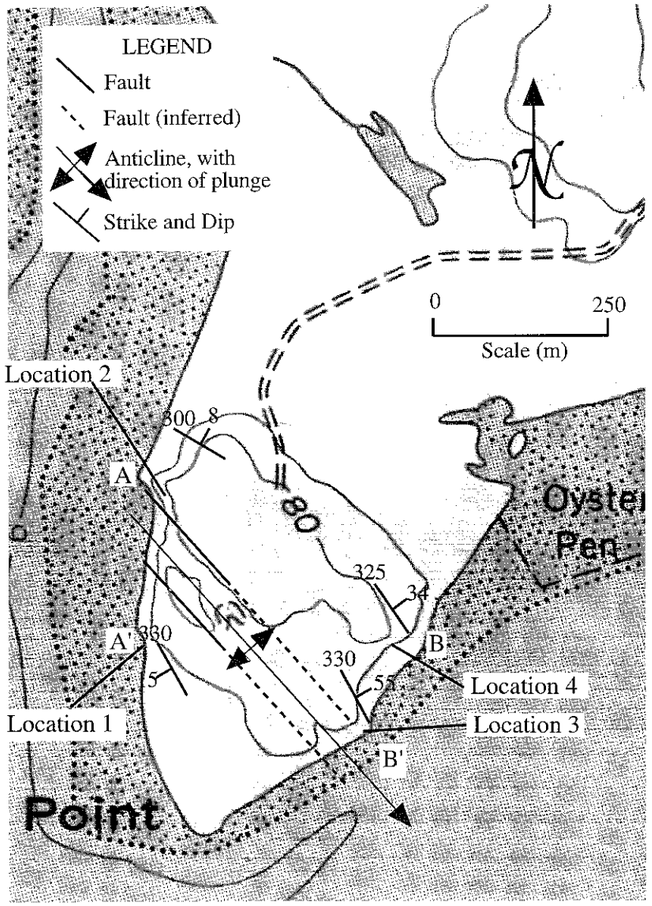

Figure 3. Topographic map of Toms Point, showing locations of cross-sections A--A' and B--B', fracture locations 1--4, and strikes and dips of bedding. Note that the axis of the south-plunging anticline lies within deformed sediments of the fault zone. Base map is USGS 7.5-minute quadrangle.

not shown on Figure 4, are massive dune sands which unconformably overlie the fluvial and estuarine sequences and which are also exposed on the southeast side of Toms Point. Pervasively sheared mud marks the northeastern most strand of the SAF on the northwest side of Toms Point. Just east of this strand is an angular unconformity between gravel beds of different ages.

Nearly vertical beds deformed by a small-scale thrust fault lie between the southwestern two fault strands (Fig. 4). There is a peat bed in the sand which is not found to the northeast and southwest of this fault block. After rainfall, there is an active spring at the location of the middle strand.

Immediately southwest of the peat bed is a mudflow and a gully which has an orientation of approximately 325°, close to the observed trend of the SAF. This is a third strand of the fault. Southwest of the mudflow is a fining-upward sequence of the Millerton Formation that is truncated against the southwestern most fault strand. The mud contains a shell layer (Fig. 4).

On the top of the Toms Point headland, between the fault traces seen on the northwest side, is a small sag pond, which was described in Lawson *et al.* (1908). The sag pond could indicate extension related to a right stepover of the fault (Brown *et al.*, 1970; Blake *et al.*, 1974), although it is at least as likely that the sediments here are weakened and gouged by faulting and simply erode away more readily.

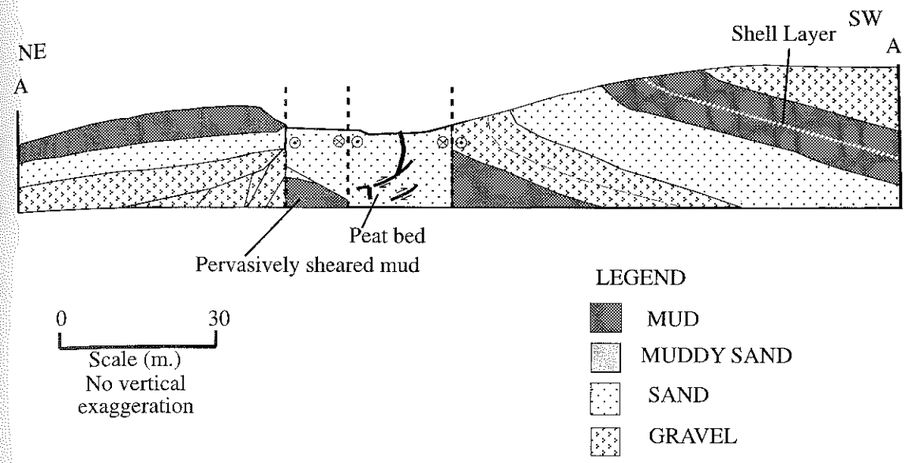

Figure 4. Cross-section of norhwest side of Toms Point headland from A to A' of Figure 3, adapted from Rutledge (1993). View is to the southeast.

Southeast Side

Figure 5 is a cross section which runs southwest to northeast from B to B' on the southeast side of Toms Point. Cliff exposures are shown in the cross section, with a covered area between them. At location B, the sediments dip gently to the northeast at approximately 30°. There is a mud layer at the base of the cliff which is overlain by a thick massive sand layer. Between the two outcrops at B and B', there is a depression approximately 110 m wide. There is a spring and lush vegetation in this depression, which may indicate that the sediments are gouged and weakened by faulting.

At location B' of Figure 3, the sediments dip to the northeast nearly 20° more steeply than the outcrop at location B. The fining-upward gravel-to-mud sequence visible on the southeast side is the same sequence exposed on the eastern end of the cliff on the northwest side. Like that sequence, the base is an angular unconformity with more steeply dipping beds of an older sequence beneath. Southwest of location B' there is heavy vegetation, and the only sediments exposed are gravels which yield little structural information. Fault strands exposed on the northwest side project into these covered gravels southwest of location B' (Figs. 3 and 5).

FRACTURE DATA AND INTERPRETATION

Fractures collected at Toms Point were divided into four main groups based on location. Figure 3 shows the locations of fracture sets on Toms Point. Most of the fracture data were collected in the mud layers, with only a few fracture sets coming from less consolidated sand layers.

Fracture orientations collected at Toms Point fall into several categories. They are primarily extension, R, and R' fractures. Fractures exhibiting plumose structures were categorized as extension fractures, and fractures that lacked indicators of motion were categorized as R or R' shear fractures based on their orientation.

Fractures measured at Toms Point show stresses that are consistent with the state of stress in a strike-slip system, in which σ_1 and σ_2 are horizontal, while σ_3 is vertical, according to Anderson's theory (Twiss and Moores, 1992).

Figure 6 is a stereoplot of theoretical fracture orientations relative to the SAF at Toms Point, which strikes at 325°. Reidel shears are conjugate sets of faults or fractures which form by the process of simple shear. The R shears are synthetic and occur at about +15° from the direction of the imposed shear; they are shown on Figure 6 at 340°. R' shears are antithetic and fall at about +75° from the direction of imposed shear. They are shown at 040°.

R and R' shear data from Toms Point show that the local stress configuration varies from the theoretical configuration. The Reidel shears appear to be rotated about 20° clockwise from the theoretical model. Reidel shears are bisected by σ_1, so the fractures from Toms Point indicate that σ_1 also lies at a greater angle from the imposed shear direction. As will be shown below, at Toms Point, fractures with plumose structures occur at approximately 050°, which is parallel to σ_1. While this stress configuration is different from the theoretical configuration, it is consistent with the state of stress along the San Andreas fault, where σ_1 is observed to be perpendicular to the fault (Zoback *et al.*, 1987).

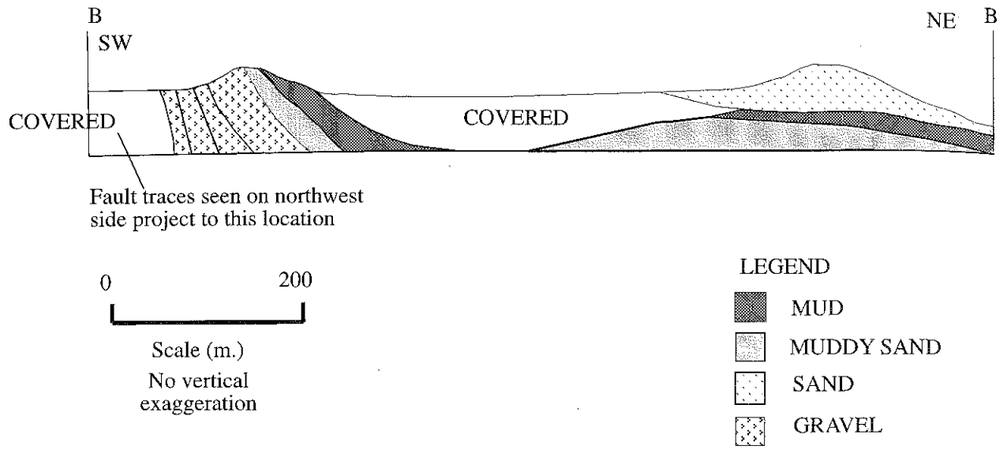

Figure 5. Cross-section of southeast side of Toms Point Headland, from B to B' of Figure 3. View is to the northwest.

Fracture Data

Most of the fractures at location 1 fall into two populations which are separated by approximately 90° (Fig. 7), suggesting they are R and R' shear fractures. There are two extension fractures, which bisect the populations of R and R' fractures at approximately 050°. The extension fractures lie parallel to σ_1 at 050°.

At location 2, plumose structures were observed on an extension fracture striking at 050° (Fig. 8). The other fractures at this location are interpreted as R or R' fractures. The R-shears strike close to north-south. The R'-shears strike closer to east-west. The state of stress inferred from these data is similar to that of location 1, with σ_1 at 050°, parallel to the extension fracture and bisecting the populations of R- and R'-shears.

Beds at location 3 of Figure 3 are separated from the beds at location 4 by a topographic low and a spring. They dip more steeply than beds at location 4, at an average of 51° NE (Fig. 9). There are two conjugate fracture sets that were measured at Location 3 and are interpreted as R and R' shear fractures. The conjugate fractures are bisected by σ_1, which lies at approximately 055°. In spite of the relatively steep dip of the beds at this location, the orientations of conjugate fractures are consistent with orientations found at locations 1 and 2, where the beds dip more gently, suggesting that both the folding of the Millerton Formation into an anticline and the fracturing of the sediments are products of fault-normal compression.

Fractures at location 4 of Figure 3 were collected in massive dune sand on the southeast side of Toms Point which overlie older fining-upwards sequences. These fractures are possibly younger than fractures measured at other locations on Toms Point. They are separated by about 60° and are interpreted as conjugate pairs (Fig. 10). The fractures suggest a stress state with σ_1 vertical, and σ_2 and σ_3 horizontal. According to Anderson's theory, this stress state is associated with normal faulting and is incompatible with the state of stress in a strike-slip system except as a local perturbation due to fault-strand geometry. The extension recorded by these fractures differs from the findings at other locations on Toms Point and could represent a component of tension where two right-lateral strike-slip faults make a right stepover. These fractures occur near a northwest-trending depression that could be the topographic expression of extension associated with a right stepover. However, exposures are not complete enough to be certain of this interpretation.

CONCLUSIONS

Exposures at Toms Point provide rare cross-sectional views of the SAF and sediments deformed by fault motions. There are three fault strands on Toms Point which can be seen clearly on the northwest side. Faults projected along strike from their exposures on the northwest side coincide with a topographic depression on the surface of the headland and with a covered interval on the southeast side.

Fractures measured at Toms Point largely fall into patterns which fit the expected state of stress for the San Andreas fault in western California. The majority of fractures are interpreted as R and R' Reidel shear fractures or extension fractures. The extension fractures strike at 050° and bisect the R and R' shear fractures. Thus the inferred principal stress direction at Toms Point from the fracture data is nearly perpendicular to the SAF and consistent with the state of stress measured at other locations along the fault. In the youngest sediments there are fracture orientations that suggest local normal faulting. One explanation for the evidence of extension at location 4 may be that it resulted from a right stepover of en echelon fault strands.

ACKNOWLEDGEMENTS

We would like to thank John Kelley of the Audobon Canyon Ranch for allowing access to Toms Point. The groundwork laid by Dave Rutledges' undergraduate thesis was of great value in this project.

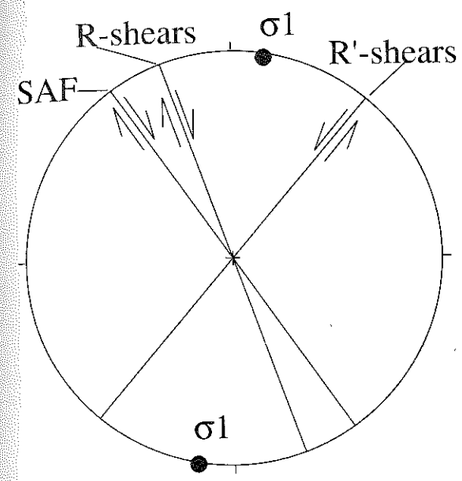

Figure 6. Stereoplot of theoretical fracture orientations. SAF = the San Andreas fault.

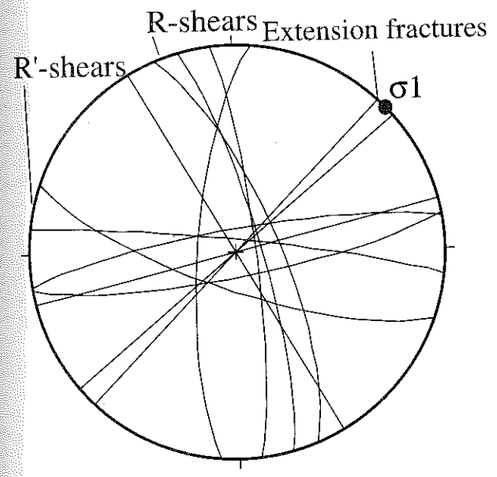

Figure 7. Fracture orientations from location 1 of Figure 3.

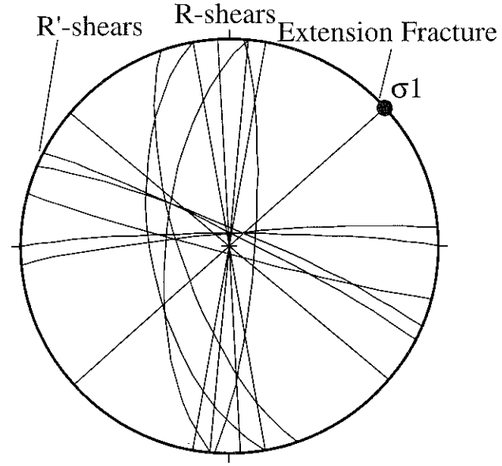

Figure 8. Fracture orientations from location 2 of Figure 3.

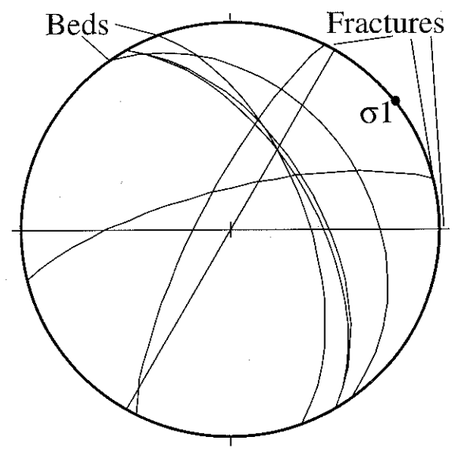

Figure 9. Fracture orientations and bedding planes from location 3 of Figure 3.

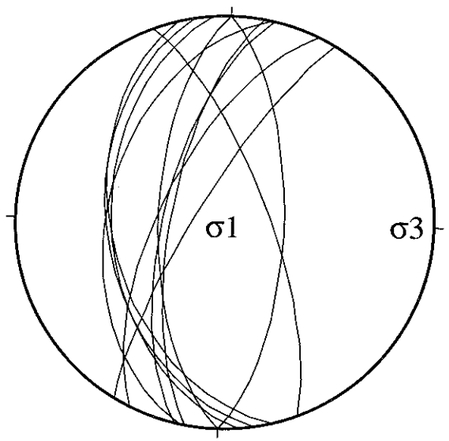

Figure 10. Fracture orientations for location 4 of Figure 3.

REFERENCES CITED

Allmendinger, R.W., 1995, Stereonet plotting computer program, version 4.9.5.

Blake, M.C., Bartow, J.A., Frizzell, V.A., Schlocker, J., Sorg, D., Wentworth, C.M., and Wright, R.H., 1974, Preliminary geologic map of Marin and San Francisco Counties and parts of Alameda, Contra Costa, and Sonoma Counties, California: United States Geological Survey Miscellaneous Field Studies Map MF574, scale 1 : 63,360.

Brown, R.D., and Wolfe, E.W., 1970, Map showing recently active breaks along the San Andreas fault between Point Delgada and Bolinas Bay, California: United States Geological Survey Map I-692, scale 1 : 48,000.

Galloway, A.J., 1977, Geology of the Point Reyes Peninsula, Marin County, California: California Division of Mines and Geology Bulletin 202, 68 pp.

Grove, K., Colson, K., Binkin, M., Dull, R., and Garrison, C., 1995, Stratigraphy and structure of the Late Pleistocene Olema Creek Formation, San Andreas fault zone north of San Francisco, California *in* Sangines, E.M, Andersen, D.W., and Buising, A.B., eds., Recent Geologic Studies in the San Francisco Bay Area: Society for Sedimentary Geology (SEPM) Pacific Section Book 76, p. 55-77.

Lawson, A.C., ed., 1908, The California earthquake of April 18, 1906, Report of State Earthquake Commission: Carnegie Institution of Washington Publication 87, 451 p.

Rutledge, D.R., 1993, Detailed structural analysis of the San Andreas fault zone at Toms Point, Tomales Bay, California: unpublished senior thesis, San Francisco State University, 20 p.

Twiss, R.J., and Moores, E.M, 1992, Structural Geology: New York,W.H. Freeman and Company, 532 p.

Wallace, R.E., 1990, The San Andreas Fault System, California: United States Geological Survey Professional Paper 1515, p. 1-80.

Zoback, M.D., Zoback, M.L., Mount, V.S., Suppe, J., Eaton, J.P., Healy, J.H., Oppenheimer, D., Reasenberg, P., Jones, L., Raleigh, C.B., Wong, I.G., Scotti, O., and Wentworth, C., 1987, New evidence on the state of stress of the San Andreas fault system: Science, v. 238, p. 1105-1111.